JOURNAL OF NEUROTRAUMA 35:105–117 (January 1, 2018)

DOI: 10.1089/neu.2017.5024

Protection against TBI-Induced Neuronal Death with Post-Treatment with a Selective Calpain-2 Inhibitor in Mice

Yubin Wang,[1] Yan Liu,[1] Dulce Lopez,[1] Moses Lee,[1] Sujay Dayal,[2] Alexander Hurtado,[1] Xiaoning Bi,[3] and Michel Baudry[1]

Abstract

Traumatic Brain Injury (TBI) is a major cause of death and disability worldwide. The calcium-dependent protease, calpain, has been shown to be involved in TBI-induced neuronal death. However, whereas various calpain inhibitors have been tested in several animal models of TBI, there has not been any clinical trial testing the efficacy of calpain inhibitors in human TBI. One important reason for this could be the lack of knowledge regarding the differential functions of the two major calpain isoforms in the brain, calpain-1 and calpain-2. In this study, we used the controlled cortical impact (CCI) model in mice to test the roles of calpain-1 and calpain-2 in TBI-induced neuronal death. Immunohistochemistry (IHC) with calpain activity markers performed at different time-points after CCI in wild-type and calpain-1 knock-out (KO) mice showed that calpain-1 was activated early in cortical areas surrounding the impact, within 0–8 h after CCI, whereas calpain-2 activation was delayed and was predominant during 8–72 h after CCI. Calpain-1 KO enhanced cell death, whereas calpain-2 activity correlated with the extent of cell death, suggesting that calpain-1 activation suppresses and calpain-2 activation promotes cell death following TBI. Systemic injection(s) of a calpain-2 selective inhibitor, NA101, at 1 h or 4 h after CCI significantly reduced calpain-2 activity and cell death around the impact site, reduced the lesion volume, and promoted motor and learning function recovery after TBI. Our data indicate that calpain-1 activity is neuroprotective and calpain-2 activity is neurodegenerative after TBI, and that a selective calpain-2 inhibitor can reduce TBI-induced cell death.

Keywords: calpain; cell death; neuroprotection; TBI

Introduction

Traumatic brain injury (TBI) is a significant public health problem in the United States. In 2010 alone, an estimated 2.5 million TBI patients presented for treatment, and it is likely that many more cases are never reported. The financial burden for the society is enormous, as many patients with TBI completely lose the ability to be self-sufficient and require long-term medical and rehabilitative care.[1] Among the different types of TBI, penetrating TBI produces the worst outcomes and highest mortality rates.[2] TBI induces immediate neuropathological consequences, which, depending on the severity, include neuronal degeneration and axonal damage.[3,4] Calpain, a family of calcium-dependent proteases regulating many cellular functions through the selective truncation of proteins,[5] has been widely shown to be involved in TBI-induced neuronal death.[6–8] As a result, numerous studies have attempted to use calpain inhibitors to reduce neuronal loss in TBI. Although several earlier studies have reported some positive effects of calpain inhibitors in animal models of TBI,[9,10] recent studies failed to confirmed these results.[11–13] An important reason that could account for these discrepancies is the incomplete knowledge regarding the differential functions of the major calpain isoforms in the brain, calpain-1 and calpain-2 (also known as μ- and m-calpain).[14]

Work from our laboratory in the last 5 years has revealed different roles of these two calpain isoforms in the brain. Specifically, we found that calpain-1 and calpain-2 play opposite functions in both synaptic plasticity and neuronal survival.[15] Calpain-1 activation is required for the initiation of theta burst stimulation-induced long-term potentiation (LTP) and is neuroprotective. On the other hand, calpain-2 activation limits the magnitude of LTP and is neurodegenerative.[16,17] The different functions of these two calpain

[1]Graduate College of Biomedical Sciences, [3]College of Osteopathic Medicine of the Pacific, Western University of Health Sciences, Pomona, California.
[2]Pitzer College, Claremont, California.

isoforms are likely the result of their differential subcellular localization and association with different signaling pathways in neurons.[15] This theory is supported by our recent finding showing that acute glaucoma-induced retinal ganglion cell (RGC) death was exacerbated in calpain-1 knock-out (KO) mice but reduced following calpain-2 inhibition,[18] and by studies showing that *CAPN1* gene deficits result in cerebellar granule cell (CGC) degeneration and cerebellar ataxia across different species including humans.[19,20] The above findings explain, at least partially, the failure of the previously tested non-isoform selective calpain inhibitors, which did not discriminate between calpain-1 and calpain-2, in many animal models of brain disorders.

In the present study, we used the controlled cortical impact (CCI) model of TBI in both wild-type (WT) and calpain-1 KO mice to assess the respective roles of calpain-1 and calpain-2 in neuronal death. We found enhanced cell death in calpain-1 KO mice, as compared with WT mice, and a linear correlation between calpain-2 activation and cell death following CCI, which confirm our previous findings that calpain-1 activation is neuroprotective, whereas calpain-2 activation is neurodegenerative. Post-TBI injection(s) of NA101, a calpain-2 selective inhibitor, significantly decreased the number of degenerating cells and lesion volume, and facilitated motor and learning function recovery after TBI. These results support the possibility of developing calpain-2 selective inhibitors as a therapeutic treatment for TBI.

Methods

Animals

Animal use in all experiments followed National Institutes of Health (NIH) guidelines and all protocols were approved by the Institution Animal Care and Use Committee of Western University of Health Sciences. Calpain-1 KO mice on a C57Bl/6 background were obtained from a breeding colony established from breeding pairs generously provided by Dr. Chishti (Tufts University). C57Bl/6 mice were purchased from Jackson Labs and were the corresponding WT. Only male mice were used in this study.

Controlled cortical impact

The CCI model was established in mice following the protocol described in previous publications.[21–24] Mice (3-month old, 25–30 g) were anesthetized using isoflurane and fixed in a stereotaxic frame with a gas anesthesia mask. A heating pad was placed beneath the body to maintain body temperature around 33–35°C. The head was positioned in the horizontal plane. The top of the skull was exposed, and a 5-mm craniotomy was made using a micro-drill lateral to the sagittal suture, and centered between bregma and lambda. The skull at the craniotomy site was carefully removed without damaging the dura. The exposed cortex was hit by a pneumatically controlled impactor device (AMS-201, Amscien). The impactor tip diameter was 3 mm, the impact velocity was 3 m/sec, and the depth of cortical deformation was 0.5 mm. After impact, the injured region was sutured using tissue adhesive (3M), and mice were placed in a 37°C incubator until they recovered from anesthesia. In sham surgery, mice were sutured after craniotomy was performed. The selective calpain-2 inhibitor, NA101, was injected as indicated at a dose of 0.3 mg/kg, based on our previous studies,[18,25] and control animals were injected with the vehicle (5% dimethyl sulfoxide [DMSO] in phosphate buffered saline [PBS]). In the case of intravenous (i.v.) injection, NA101 was injected immediately before TBI, due to the relatively low success rate of i.v. injection in this strain of mice (calpain-1 KO on a C57Bl/6J background).

Immunohistochemistry

At the indicated times after TBI, mice were anesthetized and perfused intracardially with freshly prepared 4% paraformaldehyde in 0.1 M phosphate buffer (PB; pH 7.4). After perfusion, brains were removed and immersed in 4% paraformaldehyde at 4°C for post-fixation, then in 15% and 30% sucrose at 4°C for cryoprotection. Three coronal frozen sections (20 μm thick) in each brain at bregma −0.58, −1.58, and −1.94 were prepared. To determine *in situ* calpain activation, sections were co-stained with rabbit anti-spectrin breakdown product (SBDP; 1:500; a gift from Dr. Saido, Riken, Japan) and mouse anti- phosphatase and tensin homolog (PTEN; 1:600; 9556, Cell Signaling)antibodies. To determine astrocyte and microglia activation after TBI, sections were immunostained with rabbit anti-glial fibrillary acidic protein (GFAP; 1:1000; AB5804, EMD Millipore) or goat anti-ionized calcium binding adapter molecule 1 (iba1; 1:500; ab5076, Abcam) antibody. Sections were first blocked in 0.1 M PBS containing 5% goat or donkey serum and 0.3% Triton X-100 (blocking solution) for 1 h, and then incubated with primary antibody(ies) prepared in blocking solution overnight at 4°C. Sections were washed 3 times in PBS (10 min each) and incubated in Alexa Fluor 488 goat anti-rabbit immunoglobulin (Ig)G, Alexa Fluor 488 donkey anti-goat IgG, and/or Alexa Fluor 594 goat anti-mouse IgG (1:500; Thermo Fisher Scientific) prepared in blocking solution for 2 h at room temperature. After three washes, sections were mounted with mounting medium containing 4′,6-diamidino-2-phenylindole henylindole (DAPI; Vector Laboratories). For quantification of SBDP and PTEN levels, three 637 μm × 637 μm areas near the lesion site in each section were imaged using confocal microscopes (Nikon C1 and Zeiss LSM-880) and analyzed. In each area, the regions proximal (0–170 μm from the lesion edge) and distal (>170 μm from the lesion edge) to the impact site were separately outlined using the ''Freehand Selection'' function of ImageJ, and mean fluorescence intensity (MFI) of SBDP or PTEN was measured. Data in all three sections from the same brain were averaged. For quantification of GFAP and iba1 levels, whole brain sections were imaged using the ''Tile Scan'' function of an LSM 510 confocal microscope (Zeiss). Three 300 μm × 300 μm areas centered 400 μm to the lesion edge on the ipsilateral side and three areas of the same size centered 700 μm to the cortical surface in the contralateral side were selected. MFI of GFAP or iba1 in each area was measured in ImageJ. Then, MFI in the contralateral side (background signal) was subtracted from MFI in the ipsilateral side. Data in all three sections from the same brain were averaged. Image acquisition and quantification were done by two persons in a blind fashion.

TUNEL and Fluoro-Jade C staining

Brains were collected at 0, 6, 24, and 72 h after TBI. Coronal frozen sections (20 μm thick) at bregma 1.54, 0.50, −0.58, −1.58, −1.94, and −2.30 were prepared. Terminal deoxynucleotidyl transferase dUTP nick end labeling (TUNEL) staining was performed in a set of sections using the ApopTag *in situ* apoptosis detection kit (S7165, Millipore). Sections were visualized under confocal microscopy (Nikon). All TUNEL-positive nuclei surrounding the lesion area in six sections of each brain were counted using the ''Analyze Particles'' function in ImageJ. Fluoro-Jade C staining was performed in the same set of sections. Sections were incubated in 0.0001% solution of Fluoro-Jade C (AG325; EMD Millipore) dissolved in 0.1% acetic acid for 10 min. Sections were visualized under confocal microscopy (Nikon). All Fluoro-Jade C-positive cells surrounding the lesion area in a set of sections of each brain were counted using ImageJ. To separately analyze cell death density in the region proximal and distal to the impact site, the regions proximal (0–170 μm from the edge of impact site) and distal (>170 μm from the edge of impact site) to the impact site

were outlined using the ''Freehand Selection'' function of ImageJ. TUNEL- or Fluoro-Jade C-positive cells in these two regions were separately counted. Image acquisition and quantification were done by two persons in a blind fashion.

Quantification of lesion volume

Brains were collected 3 or 30 days after TBI. Coronal frozen sections at eight different levels (bregma 1.54, 0.50, −0.58, −1.58, −1.94, −2.30, −2.70, and −3.40 mm) were prepared and stained with 0.2% cresyl violet solution (sc-214775; Santa Cruz Biotechnology) for 5 min. Sections were visualized under a light microscope (Zeiss). The lesion in each section was outlined and the lesion area was measured in ImageJ. The lesion volume between two successive sections was calculated as the average of the lesion areas of these two sections multiplied by the distance between them. The total lesion volume was the sum of lesion volumes between all the analyzed sections. Image acquisition and quantification were done by two persons in a blind fashion.

Beam walking

The beam apparatus consists of a 1-m wooden round beam with a diameter of 2 cm resting 50 cm above the tabletop on two poles. A black box is placed at the end of the beam as the finish point. Nesting material from home cages is placed in the black box to attract the mouse to the finish point. A lamp (with 60-W light bulb) is used to shine light above the start point and serves as an aversive stimulus. Each mouse is placed on a brightly lit platform and is allowed to transverse the round beam. A nylon hammock is stretched below the beam, about 7.5 cm above the table top, to cushion any falls. On training day, mice are allowed to cross the beam, with gentle guiding or prodding as needed, until they cross readily. The timer is started by the nose of the mouse entering the start point, and stopped when the animal reaches the safe box. Mice rest for 10 min in their home cages between training sessions. Mice are trained for 2 days and 3 times per day. Training is continued for additional days if mice still do not traverse the entire beam successfully after 2 days of training. The beams and box are cleaned of mouse droppings and wiped with towels soaked with 70% ethanol and then water before the next mouse is placed on the apparatus. On testing day, mice are placed on the beam and numbers of back paw slips and latency to cross are scored. Mice are tested 3 times with 10 min interval for resting. Results for the three tests are averaged to provide individual values for each mouse on that day. The experiments were performed and results analyzed by a ''blind'' observer.

Fear conditioning

Fear conditioning was performed as previously described.[26] Mice were put in the same room 30 min before being placed in the fear-conditioning chamber (H10-11MTC; Coulbourn Instruments). The conditioning chamber was cleaned with 10% ethanol to provide a background odor. A ventilation fan provided a background noise at $\sim$55 dB. After a 2-min exploration period, three tone-footshock pairings separated by 1 min intervals were delivered. The 85 dB 2 kHz tone lasted 30 sec and co-terminated with a footshock of 0.75 mA and 2 sec. Mice remained in the training chamber for another 30 sec before being returned to home cages. Context test was performed one day after training in the original conditioning chamber with 5-min recording. On day 3, animals were subjected to cue/tone test in a modified chamber with different texture and color, odor, background noise, and lighting. After 5-min recording, mice were exposed to a tone (85 dB, 2 kHz) for 1 min. Mouse behavior was recorded with the Freezeframe software and data were analyzed using the Freezeview software (Coulbourn Instruments). Motionless bouts lasting more than 1 sec were considered as freezing. The percent of time the animal froze was calculated and group means with standard error of the mean (SEM) and cumulative distribution of percent freezing were analyzed. The experiments were performed and results analyzed by a ''blind'' observer.

Results

Different time courses for calpain-1 and calpain-2 activation after TBI

To determine the levels of *in situ* activation of the two major calpain isoforms in the brain following CCI, we performed IHC to label SBDP, a calpain activity marker generated by calpain-1 and calpain-2 truncation of αII-spectrin,[27] in brain sections of WT and calpain-1 KO mice collected at multiple time-points after CCI. SBDP levels in WT mice reflect the combined activity of both calpain-1 and calpain-2, whereas in calpain-1 KO mice they reflect only calpain-2 activation. There was a significant increase in SBDP levels at 2, 6, 8, 24, and 72 h after CCI around the lesion site in WT mice, whereas in KO mice SBDP levels were not significantly elevated until 8 h after CCI. In addition, there was no significant difference in SBDP levels between WT and KO mice at 24 and 72 h after CCI (Fig. 1A,D). These results suggest a rapid and transient activation of calpain-1 (yellow dotted line in Fig. 1D), and a delayed and prolonged activation of calpain-2 (blue line in Fig. 1D) following TBI, and that calpain-2 activity is predominant starting 8 h after TBI. High-magnification images showed the distribution of SBDP in dendrites of cortical neurons and in both cell bodies and dendrites of hippocampal pyramidal neurons in the side ipsilateral to the injury (Fig. 1B,C). To verify this result, we performed IHC with an antibody against PTEN in the same set of brain sections. PTEN is a selective substrate for calpain-2 and decrease in PTEN-immunoreactivity (PTEN-ir) reflects calpain-2 activation.[18,25] Changes in PTEN-ir exhibited a similar time course in WT and KO mice. In both genotypes, PTEN-ir was significantly decreased starting at 8 h, reached a maximum decrease at 24 h after CCI (decreased by 73.5% and 67.3%, as compared with 0 h in WT and KO, respectively), and slowly recovered but was still significantly decreased at 72 h (Fig. 1A,E). The decreases in PTEN-ir in WT and KO mice (Fig. 1E) were inversely correlated with the increases in SBDP levels in KO mice (Fig. 1D), therefore reflecting the time course of calpain-2 activation after CCI.

Calpain-1 activation suppresses, whereas calpain-2 activation promotes cell death after TBI

To compare the time course of cell death following TBI in WT and KO mice, TUNEL staining was performed in brain sections (six coronal sections of each brain) of WT and calpain-1 KO mice collected at multiple time-points after CCI. The number of TUNEL-positive cells around the impact site in WT mice was not significantly increased until 24 h after CCI (Fig. 2A,B). However, the number of TUNEL-positive cells in KO mice was found significantly increased as early as 6 h after CCI. Comparing TUNEL-positive cells in WT and KO mice at each time-point, the numbers of TUNEL-positive cells were significantly higher in KO mice than in WT mice at 2, 6, 8, and 24 h but not at 72 h after CCI (Fig. 2A,B). In addition, lesion volume measured at 3 days after CCI was significantly larger in KO mice, as compared with WT mice (10.7 ± 1.4 vs. 7.5 ± 0.5, means ± SEM, $p < 0.05$; Fig. 2C,D), which is consistent with the TUNEL results. These results suggest that loss of calpain-1 activity exacerbates TBI-induced brain damage in mice.

To better understand the relationship between calpain activity and cell death following TBI, levels of SBDP or PTEN around the

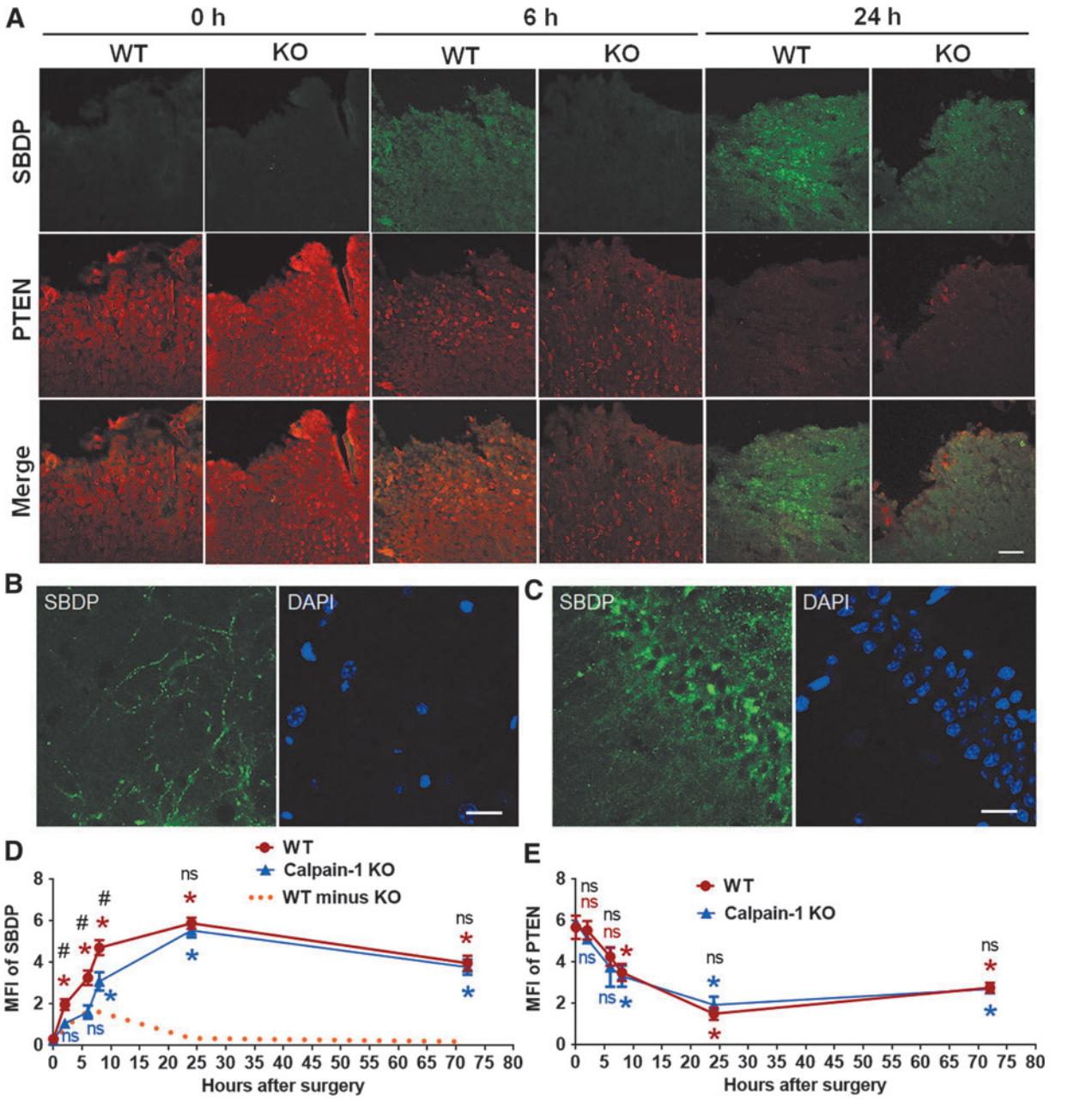

FIG. 1. Time course of calpain-1 and calpain-2 activation around the lesion site after traumatic brain injury (TBI). **(A)** Immunostaining of spectrin breakdown product (SBDP) and phosphatase and tensin homolog (PTEN) around the lesion site at various times after TBI in WT and calpain-1 knock-out (KO) mice. Scale bar, 100 μm. **(B,C)** High-magnification images of SBDP staining in ipsilateral cortex (B) and hippocampal CA1 area (C). Scale bar = 20 μm. **(D,E)** Quantification of mean fluorescence intensity (MFI) of SBDP or PTEN around the lesion site at 0, 2, 6, 8, 24, and 72 h after TBI in wild-type (WT) and KO mice. Three brain sections (bregma −0.58, −1.58, and −1.94 mm) in each animal were analyzed and MFI values averaged to provide the animal value. Data are means ± standard error of mean (SEM). For WT in Panel B, $n = 3$ at 0, 2, and 6 h, 5 at 8 and 72 h, and 6 at 24 h. For KO in Panel B, $n = 3$ at 0 and 6 h, 4 at 2 h, 5 at 8 and 72 h, and 6 at 24 h. For both WT and KO in Panel C, $n = 3$ at 0, 2, and 6 h, 4 at 24 and 72 h, and 5 at 8 h. Two KO mice died between 24 and 72 h after TBI and were removed from the experiments. $*p < 0.05$ against t = 0. One-way analysis of variance (ANOVA) followed by Bonferroni test. $\#p < 0.05$ WT versus KO at the same time-point. Two-tailed *t* test. The predicted time course of calpain-1 activity was calculated by subtracting KO SBDP signal from WT SBDP signal, and is indicated as the orange dashed line. NS, no significant difference.

lesion site in each individual animal were plotted against the numbers of TUNEL-positive cells around the lesion site in the same animal (Fig. 3). Thus, each point in Figure 3 represents one animal tested at one of the time-points shown in Figure 1 and 2. Interestingly, cell death was highly correlated ($r^2 = 0.89$ in linear regression analysis) with SBDP levels in KO mice, representing calpain-2 activity, whereas the correlation was not as prominent ($r^2 = 0.67$) in WT mice, where SBDP levels represent the combined activation of calpain-1 and calpain-2 (Fig. 3A–C). In addition, cell death was also highly correlated with PTEN levels in WT ($r^2 = 0.74$) and KO

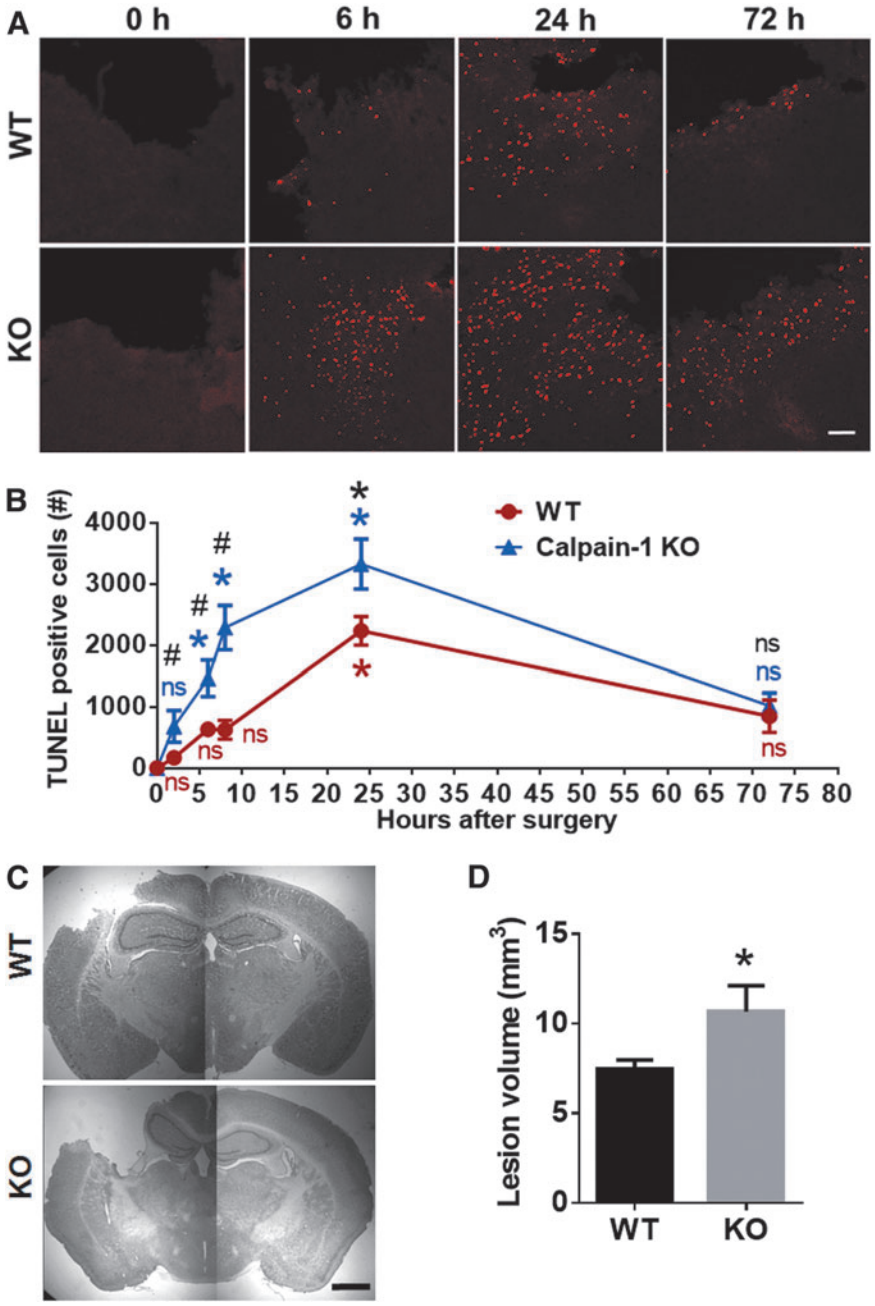

FIG. 2. Enhanced cell death and lesion size after traumatic brain injury (TBI) in calpain-1 knock-out (KO) mice, as compared with wild-type (WT) mice. **(A)** Terminal deoxynucleotidyl transferase dUTP nick end labeling (TUNEL)-positive cells around the lesion site in WT and calpain-1 KO mice at 0, 6, and 24 h and 72 h after TBI. Scale bar, 100 um. **(B)** Quantification of the number of TUNEL-positive cells around the impact site at 0, 2, 6, 8, 24, and 72 h after TBI in WT and calpain-1 KO mice. Total numbers of TUNEL-positive cells around the impact site in six sections (bregma 0.50, −0.58, −1.58, −1.94, −2.30, −2.70 mm) of each brain were counted and averaged to provide the total numbers of TUNEL-positive cells for each animal. Data are means ± standard error of mean (SEM). $N = 4$ for WT at 24 h. $N = 3$ for all other time-points in WT and KO. $*p < 0.05$ against t = 0. One-way analysis of variance (ANOVA) followed by Bonferroni test. $\#p < 0.05$ WT versus KO at the same time-point. Two-tailed t test. **(C)** Representative images of Nissl-stained brain sections (bregma −1.58 mm) in WT and KO mice collected 3 days after TBI. Scale bar, 1 mm. **(D)** Lesion volume in WT and KO mice measured 3 days after TBI. Lesion areas were measured in eight brain sections (bregma 1.54, 0.50, −0.58, −1.58, −1.94, −2.30, −2.70 and −3.40 mm) from each animal. Total lesion volume for each animal was calculated based on the lesion area in each section and the distance between sections (see Methods). $N = 8$ for WT. $N = 4$ for KO. Three KO mice died before day 3 and were removed from the experiments. $*p < 0.05$. Two-tailed t test. NS, no significant difference.

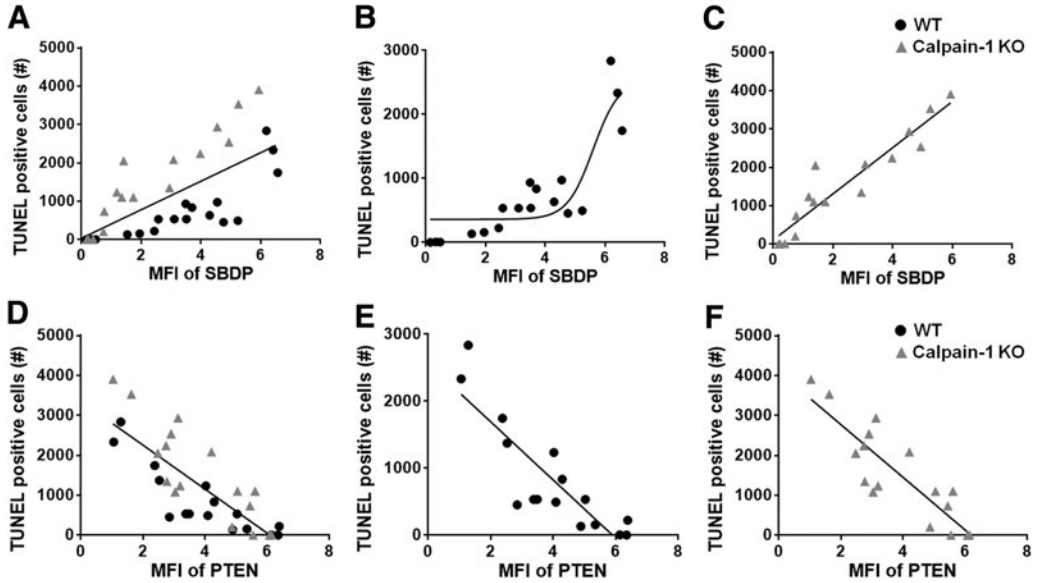

FIG. 3. Correlation between calpain-2 activity and cell death. **(A–C)** The number of terminal deoxynucleotidyl transferase dUTP nick end labeling (TUNEL)-positive cells around the site of impact at various time-points is plotted against spectrin breakdown product (SBDP) levels in both wild-type (WT) and calpain-1 knock-out (KO) mice (A), WT mice (B; $r^2 = 0.67$ in linear regression analysis), and KO mice (C; $r^2 = 0.89$). **(D–F)** The number of TUNEL-positive cells around the site of impact at various time-points is plotted against the level of full-length phosphatase and tensin homolog (PTEN) in both WT and calpain-1 KO mice (D), WT mice (E; $r^2 = 0.74$), and KO mice (F; $r^2 = 0.75$).

mice ($r^2 = 0.75$), which reflect calpain-2 activity (Fig. 3D–F). These results suggest that level of calpain-2 activation determines the extent of cell death around the lesion site after TBI.

Post-injection of NA101 inhibits calpain-2 activation after TBI

We previously identified a selective calpain-2 inhibitor, Z-Leu-Abu-CONH-CH_2-C_6H_3 (3, 5-$(OMe)_2$),[16–18,28] referred to as NA101. It has a Ki of 25 nM against calpain-2 versus a Ki of 1.3 μM against calpain-1, indicating that it has more than a 50-fold selectivity for calpain-2 over calpain-1.[17] Intraperitoneal (i.p.) injection of NA101 (0.3 mg/kg) selectively inhibited calpain-2-mediated cleavage of PTEN and STEP without affecting calpain-1-mediated cleavage of PHLPP1 in hippocampus and retina, suggesting it selectively inhibited brain calpain-2 at this dose.[18,28] In the present study, we tested the effects of NA101 at the same dose on TBI-induced calpain-2 activation in brain. Because calpain-2 activation was not significant until 8 h and reached a peak 24 h after TBI (Fig. 1), we injected NA101 (0.3 mg/kg) i.p. at 1 or 4 h after TBI and tested calpain-2 activation 24 h after TBI by examining SBDP and PTEN-ir around the lesion site. SBDP levels were significantly reduced (by 36% [1 h] and 32% [4 h], as compared with vehicle-treated mice) and PTEN levels significantly increased (by 170%, as compared with vehicle-treated mice) after NA101 injection, as compared with vehicle injection (Fig. 4A,B,D), indicating that systemic injection of NA101 results in inhibition of TBI-induced calpain-2 activation around the lesion site. NA101 injection at 1 and 4 h post-TBI showed a similar inhibitory effect on SBDP signal (Fig. 4B). Further analysis showed that after NA101 injection, SBDP levels were significantly reduced, whereas PTEN levels were increased in areas relatively distal from the lesion edge (>170 μm from the edge), but were not changed in areas closed to the lesion edge (0–170 μm from the edge; Fig. 4A,C,E), suggesting that, under our conditions, systemic NA101 injection cannot inhibit calpain-2 activation at the very edge of the lesion.

We also tested the effects of i.v. injection of NA101 on TBI-induced calpain-2 activation in cortex. NA101 (0.3 mg/kg) or vehicle was injected i.v. into calpain-1 KO mice through tail veins. TBI was immediately performed after successful injection, and levels of SBDP and full-length spectrin in cortex were examined 24 h after TBI using Western blot (Fig. 4F). NA101 significantly reduced calpain-2 mediated spectrin cleavage after TBI (by 69%, as compared with vehicle; Fig. 4G), suggesting that i.v. injection of NA101 can also inhibit calpain-2 activation in brain.

Post-TBI injection(s) of NA101 reduces TBI-induced brain damage

To determine whether calpain-2 inhibition by NA101 affects cell survival after TBI, we performed TUNEL staining in brain sections collected 24 h after TBI. Systemic injection of NA101 at either 1 or 4 h after TBI significantly reduced the number of TUNEL-positive cells around the lesion area, as compared with vehicle injection (by 41% [1 h] and 34% [4 h], as compared with vehicle; Fig. 5A,B). Further analysis of TUNEL-positive cell distribution showed that after NA101 injection, TUNEL-positive cells were limited to the edge of the lesion site (0–170 μm from the edge), in contrast to the wide-spread distribution of TUNEL-positive cells after vehicle injection (Fig. 5A,C). This distribution pattern is consistent with the spatial distribution of calpain-2 activity after NA101 injection (Fig. 4A,C,E). To verify the TUNEL results, the same set of brain sections were stained with Fluoro-Jade C, another marker for cell degeneration. NA101 injection at either 1 or 4 h after TBI significantly reduced the number of Fluoro-Jade C-positive cells around the lesion area, as compared with vehicle injection (by 39% [1 h] and 24% [4 h], as compared with vehicle; Fig. 5D,E), consistent with the TUNEL

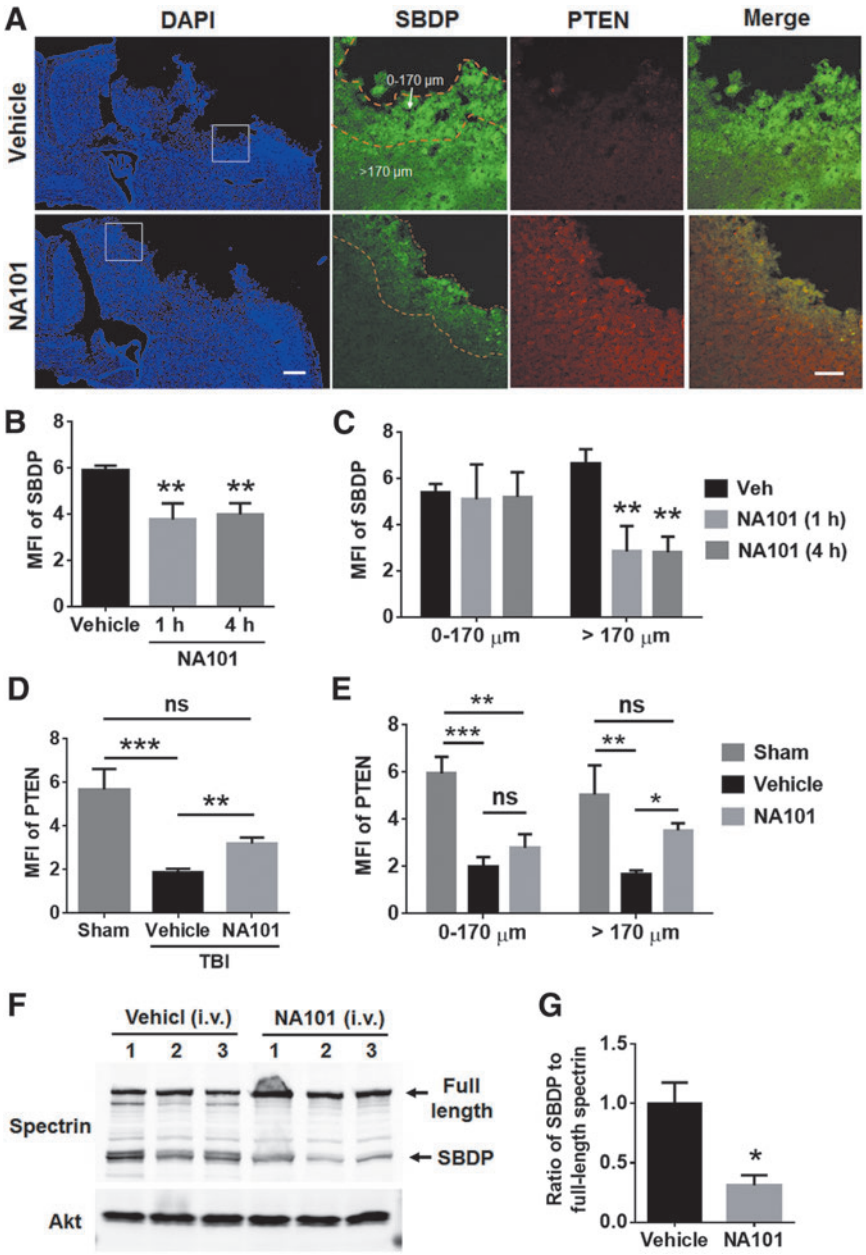

FIG. 4. Post-injection of NA101 inhibits traumatic brain injury (TBI)-triggered calpain-2 activation around the lesion site. **(A)** Immunostaining of spectrin breakdown product (SBDP) and phosphatase and tensin homolog (PTEN) 24 h after TBI in wild-type (WT) mice. Left: 4',6-diamidino-2-phenylindole (DAPI) images at low magnification; Right: high-magnification images showing changes in SBDP and PTEN. NA101 (0.3 mg/kg) was injected intraperitoneally (i.p.) 1 h after TBI. Note that NA101 reduced SBDP level in the area distal from the impact site (>170 μm) but not in the edge of the impact site (0–170 μm). Left scale bar, 500 μm. Right scale bar, 100 μm. **(B–C)** Quantification of the mean fluorescence intensity (MFI) of SBDP 24 h after TBI in mice injected with NA101 (i.p., 0.3 mg/kg) or vehicle (5% dimethyl sulfoxide [DMSO] in phosphate buffered saline [PBS]). NA101 injection either 1 or 4 h after TBI significantly reduced SBDP levels around the lesion site (B). Specifically, NA101 injection significantly reduced SBDP level in the area distal from the impact site (>170 μm) but not in the edge of the impact site (0–170 μm) (C). Data are means ± standard error of mean (SEM). $N = 9$ for vehicle, 4 for 1 h, and 5 for 4 h. $^{**}p < 0.01$ against vehicle. One-way analysis of variance (ANOVA; B) or two-way ANOVA (C) followed by Bonferroni test. **(D–E)** Quantification of MFI of full-length PTEN around the lesion site 24 h after TBI or sham surgery. NA101 or vehicle was injected 1 h after TBI. NA101 injection significantly increased PTEN levels around the lesion site, as compared with vehicle injection (D). Specifically, NA101 injection significantly increased PTEN level in the area distal from the impact site (>170 μm) but not in the edge of the impact site (0–170 μm; E). Data are means ± SEM. $N = 3$ for sham and 5 for vehicle and NA101. $^{*}p < 0.05$, $^{**}p < 0.01$, $^{***}p < 0.001$; One-way ANOVA (D) or two-way ANOVA (E) followed by Bonferroni test. **(F)** TBI was performed immediately after i.v. (intravenous) injection of NA101 (0.3 mg/kg, tail vein) or vehicle (5% DMSO in PBS) to calpain-1 KO mice. Ipsilateral cortical tissue was collected 24 h after TBI. Tissue was homogenized and aliquots of homogenates were processed for Western blot. Each lane represents tissue sample from one individual animal. **(G)** Intravenous (i.v.) injection of NA101 significantly reduced the ratio of SBDP to full-length spectrin in cortex. $N = 3$ (animals). $^{*}p < 0.05$. Two-tailed t test. ns, no significant difference.

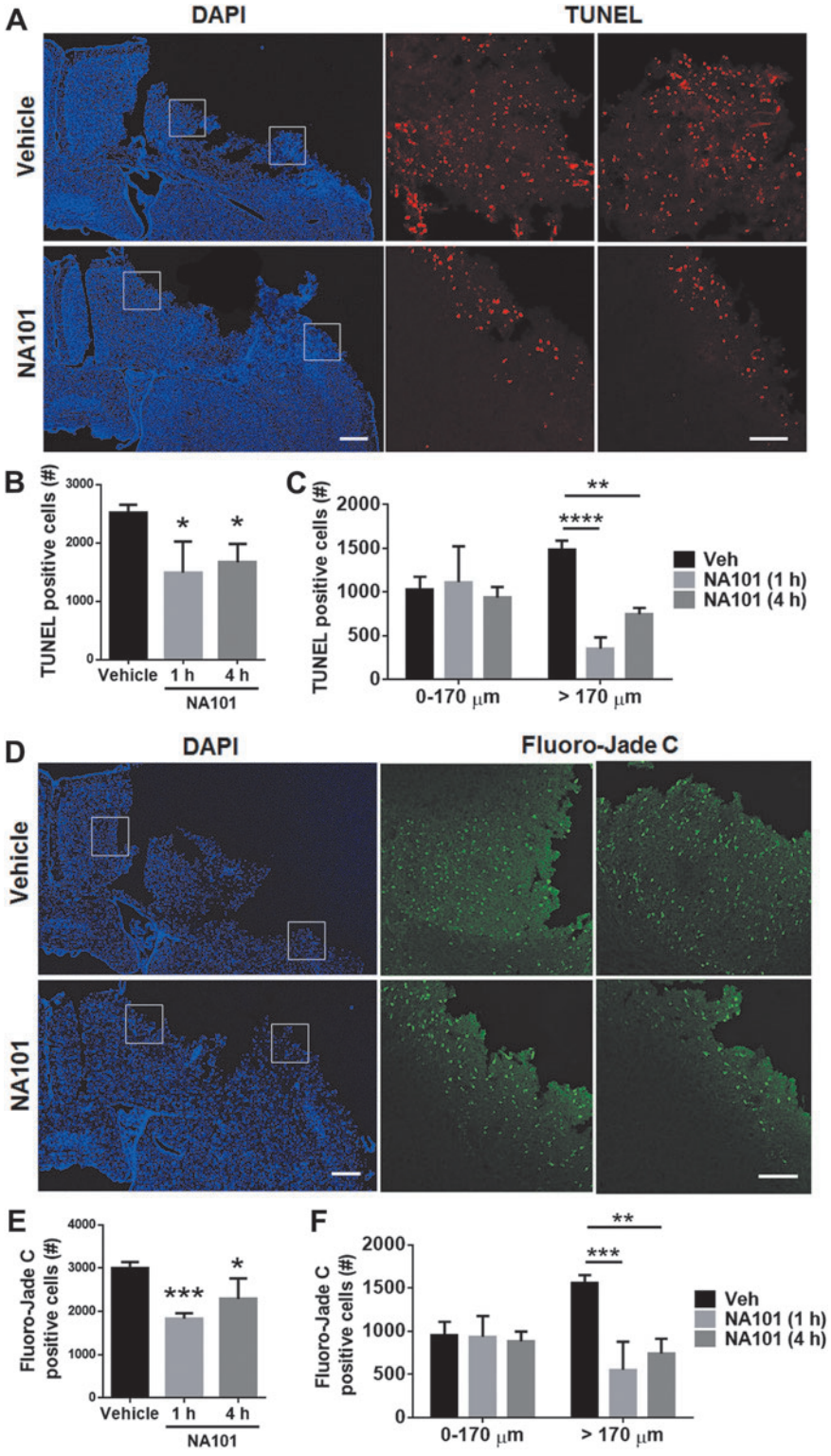

FIG. 5. Post-TBI (traumatic brain injury) injection of NA101 reduces cell death around the lesion area caused by TBI. **(A)** Terminal deoxynucleotidyl transferase dUTP nick end labeling (TUNEL) staining 24 h after TBI in the ipsilateral side of the brain in wild-type (WT) mice. Vehicle or NA101 (0.3 mg/kg) was injected 1 h after TBI. Left scale bar, 500 μm. Right scale bar, 100 μm. **(B–C)** Quantification of TUNEL staining. NA101 injection either 1 or 4 h after TBI significantly reduced the number of TUNEL-positive cells around the lesion site, as compared with vehicle injection (B). Specifically, NA101 injection significantly reduced TUNEL-positive cells in the area distal from the impact site (>170 μm) but not in the edge of the impact site (0–170 μm) (C). Data are means ± standard error of mean (SEM). $N = 9$ for vehicle, 4 for 1 h and 5 for 4 h. One mouse with NA101 injection 1 h after TBI died and was removed from the experiment.*$p < 0.05$, **$p < 0.01$, ****$p < 0.0001$ against vehicle. One-way analysis of variance (ANOVA) followed by Bonferroni test. **(D)** Fluoro-Jade C staining 24 h after TBI. Vehicle or NA101 was injected 1 h after TBI. Left bar, 500 μm. Right bar, 100 μm. **(E–F)** Quantification of Fluoro-Jade C staining. NA101 injection either 1 or 4 h after TBI significantly reduced the number of Fluoro-Jade C-positive cells around the lesion site, compared with vehicle injection (E). Specifically, NA101 injection significantly reduced the number of TUNEL-positive cells in the area distal from the impact site (>170 μm) but not in the edge of the impact site (0–170 μm; F). Data are means ± standard error of mean (SEM). $N = 7$ for vehicle, 6 for 1 h and 5 for 4 h.*$p < 0.05$, **$p < 0.01$, ***$p < 0.001$ against vehicle. One-way analysis of variance (ANOVA) followed by Bonferroni test.

results. The distribution of Fluoro-Jade C-positive cells after NA101 injection was also similar to that found with TUNEL staining. Fluoro-Jade C-positive cells were also restricted to the lesion edge after NA101 injection (Fig. 5D,F).

A single i.p. injection of NA101 (0.3 mg/kg) at either 1 or 4 h after TBI significantly reduced lesion volumes examined 3 days after TBI, as compared with vehicle injection (by 66% [1 h] and 25% [4 h, as compared with vehicle; Fig. 6A,B). However, a single injection of NA101 1 h after TBI failed to provide long-term protective effect, as there was no significant difference in lesion volume 1 month after TBI (Fig. 6C,D). On the other hand, repeated injections of NA101 (0.3 mg/kg) once a day for 8 days with the first injection at 1 h after TBI significantly reduced lesion volume 1 month after TBI, as compared with vehicle injections (by 42%, as compared with vehicle; Fig. 6C,D). Note that lesion volume significantly increased between 3 days and 1 month after TBI, indicating that processes initiated by TBI continue to lead to cell death for many days after TBI.

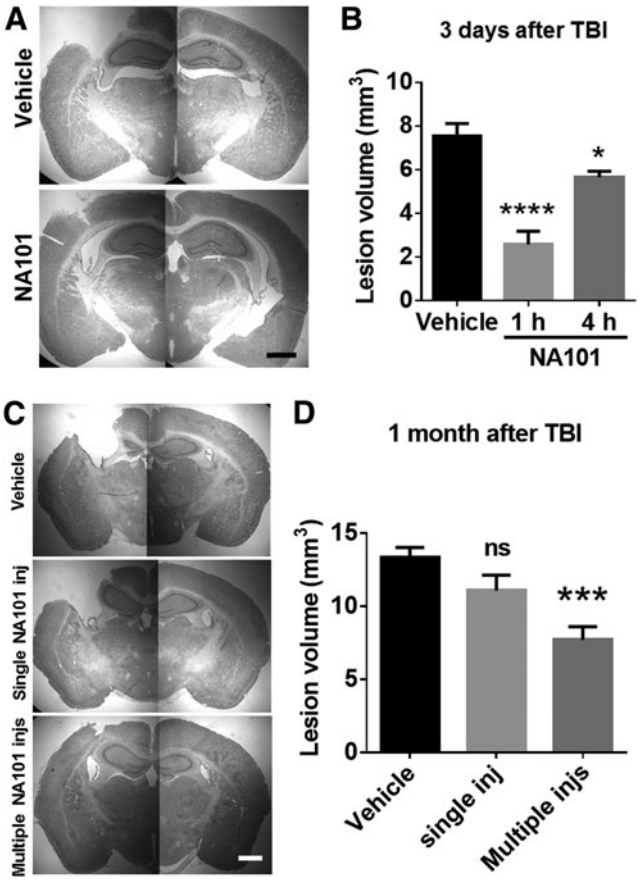

FIG. 6. Single or multiple post-injections of NA101 reduce lesion volume after traumatic brain injury (TBI). **(A)** Representative images of Nissl-stained brain sections (bregma −1.94 mm) in wild-type (WT) mice collected 3 days after TBI. NA101 (0.3 mg/kg) or vehicle (5% dimethyl sulfoxide [DMSO]) was injected intraperitoneally (i.p.) 1 h after TBI. Scale bar = 1 mm. **(B)** Lesion volume measured 3 days after TBI. NA101 or vehicle was injected once at 1 or 4 h after TBI. $N = 6$ for vehicle. $N = 5$ for NA101 injected at 1 h. $N = 6$ for NA101 injected at 4 h. $^{*}p < 0.05$, $^{****}p < 0.0001$ against vehicle. One-way analysis of variance (ANOVA) followed by Bonferroni test. **(C)** Representative images of Nissl-stained brain sections (bregma −1.58 mm) collected 30 days after TBI. Vehicle, 5% DMSO (10 mL/kg) was injected either once 1 h after TBI or once each day during day 0–7 after TBI. Single NA101 inj: NA101 was injected once (0.3 mg/kg) at 1 h after TBI. Multiple NA101 injs: NA101 was injected once each day (0.3 mg/kg) during day 0–7 after TBI. The first injection was 1 h after TBI. Scale bar = 1 mm. **(D)** Lesion volume was measured 30 days after TBI. $N = 18$ for vehicle injection(s). $N = 12$ for single NA101 injection. $N = 10$ for multiple NA101 injections. $^{***}p < 0.001$. One-way ANOVA followed by Bonferroni test. ns, no significant difference against vehicle.

Astrocyte and microglia activations are important events following TBI and also influence neuronal survival.[29,30] Thus, we examined whether post-TBI injection of NA101 could affect TBI-induced astrocyte and microglia activation. NA101 (0.3 mg/kg) or vehicle was injected i.p. once a day during days 0–7 after TBI. Brain sections were collected at day 7 and labeled with an antibody against the astrocyte marker GFAP or the microglia marker, iba1. The densities of both GFAP-and iba1-immunopositive cells were significantly increased in the side ipsilateral to the impact on day 7, as compared with day 0 after TBI (Fig. 7), confirming previous results indicating proliferation of astrocytes and microglia after TBI. High-magnification images of stained astrocytes and microglia also confirmed that both types of glial cells had acquired the typical morphology of activated cells, with enlargement of cellular processes, at day 7 after TBI. NA101 injections did not change the density or morphology of GFAP- or iba1-labeled cells on day 7, as compared with vehicle injections (Fig. 7), suggesting that NA101 has no effect on astrocyte or microglia activation after TBI.

Post-TBI injection(s) of NA101 promotes motor and learning function recovery after TBI

Motor deficit and recovery after TBI were evaluated with the beam walking test. The latency to cross and the number of footslips of the left hindlimb (contralateral to the injury) were analyzed, as mice walked across a 1 m-long round beam. Mice were tested on day 1, 2, 3, 4, and 8 after TBI or sham surgery. NA101 (0.3 mg/kg) or vehicle was injected once 1 h after TBI. There was no significant difference in time to cross or number of footslips between NA101- and vehicle-treated groups on day 1 (Fig. 8A,B). However, animals in the NA101 group rapidly recovered to levels similar to those in naive and sham groups, whereas animals in the vehicle group recovered much slower. Time to cross was significantly shorter on day 3, 4, and 8 in the NA101 group, as compared with the vehicle group (Fig. 8A). Number of footslips was significantly lower on day 2 and 8 in the NA101 group, as compared with the vehicle group (Fig. 8B). In addition, when NA101 was repeatedly injected once a day during day 0–7 after TBI, motor function was significantly improved at day 8 after TBI, as compared with repeated vehicle injections (Fig. 8C,D). These results suggest that either a single post-TBI injection or repeated post-TBI injections of NA101 promote motor function recovery after TBI in mice.

To determine whether NA101 could reverse TBI-induced learning impairment, we used the fear-conditioning paradigm. NA101 or vehicle was repeatedly injected once a day during day 0–7 after TBI. Mice were trained on day 10 after TBI, and contextual and cued fear conditioning were tested on day 11 and 12. TBI impaired context-dependent but not tone-dependent learning, and NA101 treatment significantly enhanced context learning after TBI (Fig. 8E,F). There was no difference in freezing time in the preconditioning period among all groups (Fig. 8E,F). This result suggests that NA101 treatment reverses TBI-induced impairment in hippocampus-dependent learning.

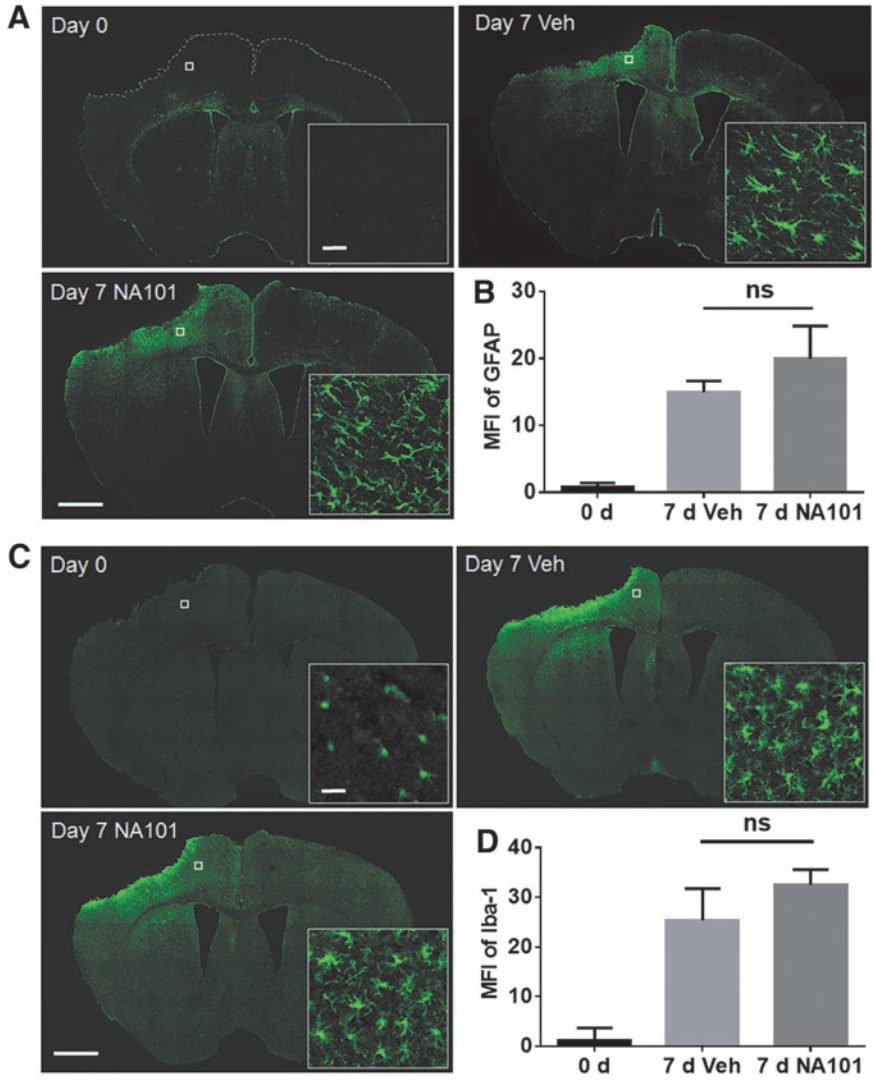

FIG. 7. Post-TBI (traumatic brain injury) injections of NA101 have no effect on TBI-induced activation of astrocytes and microglia. **(A)** Immunostaining of coronal brain sections with glial fibrillary acidic protein (GFAP). Day 0: brain sections were collected immediately after TBI. Day 7 Veh: vehicle (5% dimethyl sulfoxide [DMSO] in phosphate buffered saline [PBS], 10 mL/kg) was injected once a day during day 0–7 after TBI and brain sections were collected at day 7. Day 7 NA101: NA101 (0.3 mg/kg) was injected once a day during day 0–7 and brain sections were collected at day 7. Scale bar (low-magnification images) = 1 mm. Scale bar (high-magnification images) = 20 μm. **(B)** Quantification of GFAP fluorescence intensity near the lesion site. Data are means ± standard error of mean (SEM). $N = 3$ (animals) in each group. Three sections (bregma −0.58, −1.58, −1.94) in each animal were analyzed and the values averaged. One-way analysis of variance (ANOVA) followed by Bonferroni test. **(C)** Immunostaining of brain sections with ionized calcium binding adapter molecule 1 (iba1). Scale bar (low-magnification images) = 1 mm. Scale bar (high-magnification images) = 20 μm **(D)**. Quantification of iba1 fluorescence intensity near the lesion site. Data are means ± standard error of mean (SEM). $N = 3$ (animals) in each group. Three sections (bregma −0.58, −1.58, −1.94) in each animal were analyzed and the values averaged. One-way ANOVA followed by Bonferroni test. Ns, no significant difference.

Discussion

Our results show that TBI is associated with activation of both calpain-1 and calpain-2 but with very different time courses and functional effects. Thus, calpain-1 is rapidly but transiently activated following TBI, and calpain-2 activation is delayed and prolonged. Moreover, whereas calpain-1 activation is neuroprotective, calpain-2 activation is neurodegenerative. Our results also show that calpain-2 activation is closely associated with cell death following TBI and that a selective calpain-2 inhibitor provides a significant degree of protection when administered systemically after TBI. Finally, they not only account for the previous conflicting results regarding the involvement of calpain in neuronal death and in particular in TBI, but also strengthen the notion that calpain-2 is a good target to develop new neuroprotective molecules.

Conflicting results with non-isoform selective calpain inhibitors in TBI

Calpain activation has long been shown to be involved in the pathology of TBI, stroke, and other chronic neurodegenerative diseases such as Alzheimer's disease (AD), Parkinson's disease (PD), and Huntington's disease (HD).[6,31] As a result, this enzyme has been an attractive therapeutic target for many years. However,

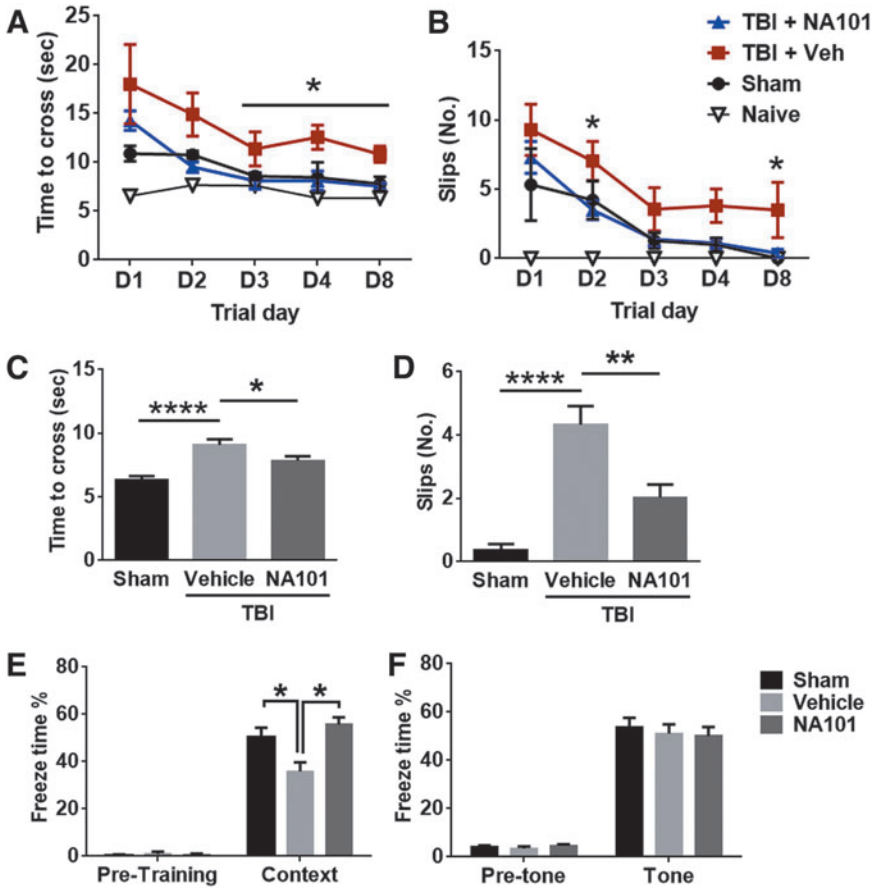

FIG. 8. Post-injection(s) of NA101 facilitates recovery of motor and learning ability after traumatic brain injury (TBI). **(A,B)** Effects of single injection of NA101 (0.3 mg/kg, injected intraperitoneally [i.p.] 1 h after TBI) or vehicle (5% dimethyl sulfoxide [DMSO]) on beam walking test following TBI. Motor function after TBI was measured by (A) time to cross the beam and (B) number of footslips from the left hindlimb (the lesion is in the right hemisphere) during day 1–8 after TBI. Data are means ± standard error of mean (SEM). $N = 8$ for TBI + NA101, 9 for TBI + vehicle, 6 for sham, and 6 for naive. One mouse with TBI plus NA101 injection and 1 mouse with sham surgery died and were removed from the experiment. $*p < 0.05$ TBI + NA101 versus TBI + vehicle at the same trial day. One-way analysis of variance (ANOVA) followed by Bonferroni test. (C,D) NA101 (0.3 mg/kg) or vehicle was injected once each day during day 0–7 after TBI. Time to cross the beam (C) and number of footslips (D) were measured at day 8 after TBI. Data are means ± standard error of mean (SEM). $N = 10$ for TBI + NA101 and TBI + vehicle. $N = 8$ for sham. $*p < 0.05$, $**p < 0.01$, $****p < 0.0001$. One-way ANOVA followed by Bonferroni test. **(E,F)** Effect of repeated injections of NA101 on fear conditioning after TBI. NA101 or vehicle was injected once each day during day 0–7 after TBI. Mice were trained on day 10 and tested for context-dependent fear conditioning on day 11 and for tone-dependent fear conditioning on day 12. Data are percent freezing in context conditioning (E) and in tone conditioning (F). Data are means ± standard error of mean (SEM). $N = 10$ for sham, 5 for vehicle, 6 for NA101. $* p < 0.05$. One-way ANOVA followed by Bonferroni test.

all the studies directed at evaluating the role of calpain in neuronal death did not address the relative activation of calpain-1 and calpain-2 and did not use isoform selective calpain inhibitors, often leading to conflicting results. In the case of TBI, two studies in the '90s reported that the calpain inhibitor AK295 protected cytoskeletal structure of injured neurons and attenuated motor and cognitive deficits after TBI.[9,10] However, recent studies using other calpain inhibitors failed to confirm the above results. In particular, overexpression of the endogenous calpain inhibitor, calpastatin, was reported to reduce calpain activation,[32] but had no effect on neuronal death.[12] Another recent study concluded that even two blood–brain barrier- and cell-permeable calpain inhibitors, SNJ-1945 and MDL-28170, did not have a sufficient efficacy and a practical therapeutic window in a model of control cortical impact.[13,33] Although non-isoform selective inhibitors were shown to inhibit overall calpain activation (without distinguishing which calpain isoform was targeted) following TBI, they failed to provide neuroprotection. Our results are in good agreement with these studies, as they show that both calpain-1 and calpain-2 are activated after TBI, but indicate that it could be difficult to predict the effects of non-selective inhibitors, as they will critically depend on the time of injection of the inhibitors. It is conceivable that delayed injection of a non-selective calpain inhibitor could be beneficial if injected late after TBI, once calpain-1 activation has terminated.

Importance of calpain subcellular localization

We previously proposed that different subcellular localizations of calpain-1 and calpain-2 are responsible, at least in part, for their different functions, with calpain-1 downstream of synaptic *N*-methyl-D-aspartate receptors (NMDARs) and calpain-2 downstream of non-synaptic NMDARs.[15] Our results support the localization hypothesis in the TBI model. Calpain-1 activation is neuroprotective, whereas calpain-2 activation is neurodegenerative

following TBI, suggesting that their activation triggers pro-survival pathway and pro-death pathway, respectively. The different time courses for calpain isoform activation and their opposite functions we observed after TBI are consistent with similar results obtained in a different model of acute neurodegeneration using increased intraocular pressure to produce retinal ganglion cell death.[18] These results suggest that the differential activation and functions of calpain-1 and calpain-2 could represent a common mechanism in brain disorders involving glutamate excitotoxicity. This pattern fits the proposed localization of calpain-1 and calpain-2. Calpain-1 is located at synapses and is promptly activated following pre-synaptic glutamate release. Calpain-2 is located at extra-synaptic sites and is activated only when extra-synaptic glutamate level increases, which occurs predominantly under pathological conditions.

It is somewhat more difficult to explain the different results reported by Yamada and colleagues,[21] who used the same calpain-1 KO mice and the same model of TBI but reported that the number of degenerating cells and the lesion volume were smaller in calpain-1 KO mice than in WT mice. It is important to note that these authors did not report the lesion volume but the volume of the remaining cortex, which is not necessarily directly related to the lesion volume. Second, the number of Fluoro-Jade-C-positive cells they report is much smaller than the number of TUNEL-positive neurons, whereas these numbers are relatively similar in our experiments. However, they labeled degenerating neurons 3 days after TBI, whereas we measured them 24 h after TBI to capture the majority of dying cells. They also indicated that the majority of the TUNEL-positive cells were observed within 100 μm from the border of the contusion cavity, whereas we observed the largest effects of the calpain inhibitor in the area beyond 170 μm from the contusion border.

Physiological roles of calpain-1 in the brain

In this study, we found that, following TBI, cell death and lesion volume were larger in calpain-1 KO mice than in WT mice. The level of the total activity of calpain-1 and calpain-2 poorly correlated with the level of cell death, whereas the level of calpain-2 activity alone exhibited a linear correlation with the number of degenerating cells (Fig. 3 B,C), suggesting that calpain-1 and calpain-2 activation have conflicting roles in determining neuronal fate. Consistent with what we found in this study, both retinal ganglion cell death following acute glaucoma and hippocampal neuronal death following kainate-induced seizure were enhanced in calpain-1 KO mice, as compared with WT mice.[18,34] Calpain-1 KO or knockdown results in neuron degeneration across different species including human, dog, mice, zebrafish, fruit fly, and Caenorhabditis elegans.[19,20] In addition, according to a recent study, calpain activation in the early phase after insult (possibly calpain-1 activity) inhibits caspase activity.[35] It is therefore possible that enhanced cell degeneration after TBI in calpain-1 KO mice may also be due to enhanced caspase activity. All these results suggest a pro-survival role of calpain-1 activity both during the post-natal period and in the adult. Another important physiological role of calpain-1 in the brain is regulating synaptic plasticity, the mechanism underlying learning and memory.[16,36,37] Thus, it is critical to avoid disrupting the physiological function of calpain-1 when targeting the calpain system for the treatment of neurodegenerative diseases.

Calpain-2 as a novel pharmaceutical target for neuronal degeneration

Our results showed that calpain-2 activation around the lesion site is not significant until 8 h after TBI, suggesting the existence of an 8-h window post-TBI during which to deliver calpain-2 inhibitors. Systemic injection of NA101 at 1 or 4 h after TBI significantly reduced calpain-2 activation around the lesion area 24 h after TBI, indicating delivery efficacy and a relatively long half-life of NA101 in mice. The decrease in calpain-2 activity by NA101 treatment correlated with the decrease in the number of degenerating cells, suggesting a pro-death role of TBI-triggered calpain-2 activation. Similarly, systemic or local application of NA101 2 h after acute glaucoma reduced calpain-2 activation and retinal ganglion cell death.[18] In addition to acute insults, calpain-2 has also been involved in the pathology of chronic neurodegenerative diseases. In particular, calpain-2 but not calpain-1 activation is concentrated in neurofibrillary tangles and induces degradation of nicotinic acetylcholine receptor α4 and causes cholinergic impairments in AD.[38,39]

Conclusion

Our results using a mouse model of TBI indicate that calpain-1 activation supports neuronal survival, whereas calpain-2 activation promotes neuronal death after TBI. Post-TBI treatment with a selective calpain-2 inhibitor provides a significant degree of neuroprotection and facilitates behavioral recovery. The opposite functions of calpain-1 and calpain-2 we observed in several acute models of insults could also participate in chronic neurodegenerative disorders, such as AD and PD, and it is tempting to speculate that selective calpain-2 inhibitors might also be beneficial in these disorders.

Acknowledgments

This work was supported by grant P01NS045260-01 from NINDS (PI: Dr. C.M. Gall), grant R01NS057128 from NINDS to M.B., and grant R15MH101703 from NIMH to X.B. X.B. is also supported by funds from the Daljit and Elaine Sarkaria Chair.

Author Disclosure Statement

Drs. Wang, Bi, and Baudry are co-founders of NeurAegis, Inc., a biotech start-up company, focusing on developing selective calpain-2 inhibitors for the treatment of acute neurodegeneration. All the other co-authors do not have conflict of interest.

References

1. Coronado, V.G., Xu, L., Basavaraju, S.V., McGuire, L.C., Wald, M.M., Faul, M.D., Guzman, B.R., and Hemphill, J.D. (2011). Surveillance for traumatic brain injury-related deaths: United States, 1997–2007. US Department of Health and Human Services, Centers for Disease Control and Prevention: Atlanta, GA.
2. Binder, S., Corrigan, J.D., and Langlois, J.A. (2005). The public health approach to traumatic brain injury: an overview of CDC's research and programs. J. Head Trauma Rehabil. 20, 189–195.
3. Gupta, R., and Sen, N. (2016). Traumatic brain injury: a risk factor for neurodegenerative diseases. Rev. Neurosci. 27, 93–100.
4. Siedler, D.G., Chuah, M.I., Kirkcaldie, M., Vickers, J.C., and King, A.E. (2013). Diffuse axonal injury in brain trauma: insights from alterations in neurofilaments. Front. Cell. Neurosci. 8, 429–429.
5. Ono, Y., and Sorimachi, H. (2012). Calpains: an elaborate proteolytic system. Biochim. Biophys. Acta. 1824, 224–236.
6. Liu, S., Yin, F., Zhang, J., and Qian, Y. (2014). The role of calpains in traumatic brain injury. Brain Inj. 28, 133–137.
7. Cagmat, E.B., Guingab-Cagmat, J.D., Vakulenko, A.V., Hayes, R.L., and Anagli, J. (2015). Chapter 40: Potential use of calpain inhibitors as brain injury therapy, in: *Brain Neurotrauma: Molecular, Neuropsychological, and Rehabilitation Aspects.* Kobeissy, FH (ed). CRC Press/Taylor & Francis: Boca Raton, FL.
8. Kobeissy, F.H., Liu, M.C., Yang, Z., Zhang, Z., Zheng, W., Glushakova, O., Mondello, S., Anagli, J., Hayes, R.L., and Wang, K.K.

(2015). Degradation of βII-spectrin protein by calpain-2 and caspase-3 under neurotoxic and traumatic brain injury conditions. Mol. Neurobiol. 52, 696–709.
9. Posmantur, R., Kampfl, A., Siman, R., Liu, J., Zhao, X., Clifton, G.L., and Hayes, R.L. (1997). A calpain inhibitor attenuates cortical cytoskeletal protein loss after experimental traumatic brain injury in the rat. Neuroscience 77, 875–888.
10. Saatman, K.E., Murai, H., Bartus, R.T., Smith, D.H., Hayward, N.J., Perri, B.R., and McIntosh, T.K. (1996). Calpain inhibitor AK295 attenuates motor and cognitive deficits following experimental brain injury in the rat. Proc. Natl. Acad. Sci. U. S. A. 93, 3428–3433.
11. Thompson, S.N., Carrico, K.M., Mustafa, A.G., Bains, M., and Hall, E.D. (2010). A pharmacological analysis of the neuroprotective efficacy of the brain-and cell-permeable calpain inhibitor MDL-28170 in the mouse controlled cortical impact traumatic brain injury model. J. Neurotrauma 27, 2233–2243.
12. Schoch, K.M., Reyn, C.R., Bian, J., Telling, G.C., Meaney, D.F., and Saatman, K.E. (2013). Brain injury-induced proteolysis is reduced in a novel calpastatin-overexpressing transgenic mouse. J. Neurochem. 125, 909–920.
13. Bains, M., Cebak, J.E., Gilmer, L.K., Barnes, C.C., Thompson, S.N., Geddes, J.W., and Hall, E.D. (2013). Pharmacological analysis of the cortical neuronal cytoskeletal protective efficacy of the calpain inhibitor SNJ-1945 in a mouse traumatic brain injury model. J. Neurochem. 125, 125–132.
14. Donkor, I.O. (2011). Calpain inhibitors: a survey of compounds reported in the patent and scientific literature. Expert Opin. Ther. Pat. 21, 601–636.
15. Baudry, M., and Bi, X. (2016). Calpain-1 and calpain-2: the yin and yang of synaptic plasticity and neurodegeneration. Trends Neurosci. 39, 235–245.
16. Wang, Y., Zhu, G., Briz, V., Hsu, Y.T., Bi, X., and Baudry, M. (2014). A molecular brake controls the magnitude of long-term potentiation. Nat. Commun. 5, 3051.
17. Wang, Y., Briz, V., Chishti, A., Bi, X., and Baudry, M. (2013). Distinct roles for mu-calpain and m-calpain in synaptic NMDAR-mediated neuroprotection and extrasynaptic NMDAR-mediated neurodegeneration. J. Neurosci. 33, 18880–18892.
18. Wang, Y., Lopez, D., Davey, P.G., Cameron, D.J., Nguyen, K., Tran, J., Marquez, E., Liu, Y., Bi, X., and Baudry, M. (2016). Calpain-1 and calpain-2 play opposite roles in retinal ganglion cell degeneration induced by retinal ischemia/reperfusion injury. Neurobiol. Dis. 93, 121–128.
19. Gan-Or, Z., Bouslam, N., Birouk, N., Lissouba, A., Chambers, D.B., Veriepe, J., Androschuck, A., Laurent, S.B., Rochefort, D., Spiegelman, D., Dionne-Laporte, A., Szuto, A., Liao, M., Figlewicz, D.A., Bouhouche, A., Benomar, A., Yahyaoui, M., Ouazzani, R., Yoon, G., Dupre, N., Suchowersky, O., Bolduc, F.V., Parker, J.A., Dion, P.A., Drapeau, P., Rouleau, G.A., and Bencheikh, B.O. (2016). Mutations in CAPN1 cause autosomal-recessive hereditary spastic paraplegia. Am. J. Hum. Genet. 98, 1038–1046.
20. Wang, Y., Hersheson, J., Lopez, D., Hammer, M., Liu, Y., Lee, K.H., Pinto, V., Seinfeld, J., Wiethoff, S., Sun, J., Amouri, R., Hentati, F., Baudry, N., Tran, J., Singleton, A.B., Coutelier, M., Brice, A., Stevanin, G., Durr, A., Bi, X., Houlden, H., and Baudry, M. (2016). Defects in the CAPN1 gene result in alterations in cerebellar development and cerebellar ataxia in mice and humans. Cell Rep. 16, 79–91.
21. Yamada, K.H., Kozlowski, D.A., Seidl, S.E., Lance, S., Wieschhaus, A.J., Sundivakkam, P., Tiruppathi, C., Chishti, I., Herman, I.M., Kuchay, S.M., and Chishti, A.H. (2012). Targeted gene inactivation of calpain-1 suppresses cortical degeneration due to traumatic brain injury and neuronal apoptosis induced by oxidative stress. J. Biol. Chem. 287, 13182–13193.
22. Smith, D.H., Soares, H.D., Pierce, J.S., Perlman, K.G., Saatman, K.E., Meaney, D.F., Dixon, C.E., and McIntosh, T.K. (1995). A model of parasagittal controlled cortical impact in the mouse: cognitive and histopathologic effects. J. Neurotrauma 12, 169–178.
23. Hall, E.D., Sullivan, P.G., Gibson, T.R., Pavel, K.M., Thompson, B.M., and Scheff, S.W. (2005). Spatial and temporal characteristics of neurodegeneration after controlled cortical impact in mice: more than a focal brain injury. J. Neurotrauma 22, 252–265.
24. Romine, J., Gao, X., and Chen, J. (2014). Controlled cortical impact model for traumatic brain injury. JoVE, e51781–e51781.
25. Briz, V., Hsu, Y.-T., Li, Y., Lee, E., Bi, X., and Baudry, M. (2013). Calpain-2-mediated PTEN degradation contributes to BDNF-induced stimulation of dendritic protein synthesis. J. Neurosci. 33, 4317–4328.
26. Sun, J., Zhu, G., Liu, Y., Standley, S., Ji, A., Tunuguntla, R., Wang, Y., Claus, C., Luo, Y., Baudry, M., and Bi, X. (2015). UBE3A regulates synaptic plasticity and learning and memory by controlling SK2 channel endocytosis. Cell Rep. 12, 449–461.
27. Seubert, P., Baudry, M., Dudek, S., and Lynch, G. (1987). Calmodulin stimulates the degradation of brain spectrin by calpain. Synapse 1, 20–24.
28. Liu, Y., Wang, Y., Zhu, G., Sun, J., Bi, X., and Baudry, M. (2016). A calpain-2 selective inhibitor enhances learning & memory by prolonging ERK activation. Neuropharmacology 105, 471–477.
29. Burda, J.E., Bernstein, A.M., and Sofroniew, M.V. (2016). Astrocyte roles in traumatic brain injury. Exp. Neurol. 275, Pt. 3, 305–315.
30. Loane, D.J., and Byrnes, K.R. (2010). Role of microglia in neurotrauma. Neurotherapeutics 7, 366–377.
31. Bezprozvanny, I. (2009). Calcium signaling and neurodegenerative diseases. Trends Mol. Med. 15, 89–100.
32. Yan, X.-X., and Jeromin, A. (2012). Spectrin breakdown products (SBDPs) as potential biomarkers for neurodegenerative diseases. Curr. Transl. Geriatr. Exp. Gerontol. Rep. 1, 85–93.
33. Thompson, S.N., Carrico, K.M., Mustafa, A.G., Bains, M., and Hall, E.D. (2010). A pharmacological analysis of the neuroprotective efficacy of the brain- and cell-permeable calpain inhibitor MDL-28170 in the mouse controlled cortical impact traumatic brain injury model. J. Neurotrauma 27, 2233–2243.
34. Seinfeld, J., Baudry, N., Xu, X., Bi, X., and Baudry, M. (2016). Differential activation of calpain-1 and calpain-2 following kainate-induced seizure activity in rats and mice. eNeuro 3, eCollection 2016.
35. Neumar, R.W., Xu, Y.A., Gada, H., Guttmann, R.P., and Siman, R. (2003). Cross-talk between calpain and caspase proteolytic systems during neuronal apoptosis. J. Biol. Chem. 278, 14162–14167.
36. Liu, J., Liu, M.C., and Wang, K. (2008). Calpain in the CNS: from synaptic function to neurotoxicity. Sci. Signal 1, re1.
37. Lynch, G., and Baudry, M. (1984). The biochemistry of memory: a new and specific hypothesis. Science 224, 1057–1063.
38. Grynspan, F., Griffin, W.R., Cataldo, A., Katayama, S., and Nixon, R.A. (1997). Active site-directed antibodies identify calpain II as an early-appearing and pervasive component of neurofibrillary pathology in Alzheimer's disease. Brain Res 763, 145–158.
39. Yin, Y., Wang, Y., Gao, D., Ye, J., Wang, X., Fang, L., Wu, D., Pi, G., Lu, C., and Zhou, X.-W. (2016). Accumulation of human full-length tau induces degradation of nicotinic acetylcholine receptor α4 via activating calpain-2. Sci. Rep. 6, 27283.

Address correspondence to:
Michel Baudry, PhD
Graduate College of Biomedical Sciences
Western University of Health Sciences
309 E. 2nd Street
Pomona, CA 91766

E-mail: mbaudry@westernu.edu